Highly Efficient Self-healing Material with Excellent Shape Memory and Unprecedented Mechanical Properties

Chaoxian Chen [1], Siwen Chen [1], Zhihao Guo [1], Wanruo Hu [1], Zhangpei Chen [1], Jiwei Wang[3, *], Jianshe Hu [1, *], Jing Guo [2], Liqun Yang [2, *]

Table of contents

The supplementary information file includes, 10 supplementary Figures (Figures S1-S10), 3 supplementary Table (Table S1-S3) and 4 supplementary movies (Movie S1-S4)

FTIR characterization

The structure of the monomer and the elastomers were characterized by Fourier transform infrared spectroscopy (ATR-FTIR). As illustrated in Figure S1 (a), the peaks at 3033, 1607(1499), and 768(696) cm^{-1} corresponded to stretching vibration of C-H on the benzene ring, stretching vibration of benzene ring skeleton and out-of-plane bending vibration of C-H on mono-substituted benzene, respectively. At the same time, MBC exhibited characteristic peaks at 1753, 1736, 1174 and 1230(1132) cm^{-1}, which corresponded to cocyclic ester carbonyl C=O double bond stretching vibration, ester carbonyl C=O double bond stretching vibration, cyclic ester stretching vibration of carbonyl C-O-C and antisymmetric and symmetrical stretching vibration of ester carbonyl C-O-C, respectively. The elastomers were shown in Figure S1 (b), it can be seen that the infrared spectra of P_1-P_4 are similar. The characteristic peaks at 3033, 1753 and 1174 cm^{-1} of the monomer were disappeared, this revealed that the monomer MBC had successfully ring-opened. Furthermore, the new peaks at 3400-3000 cm^{-1} have appeared, and the peaks of the benzene ring of elastomers were enhanced, which indicated that the hydroxyl and hydrophobic associations of elastomers were established. Accordingly, the self-healing properties of the dual-physical cross-links of the elastomers were formed.

Thermogravimetric analysis

The TGA curves of the P_1-P_4 elastomers with different catalyst were shown in Figure S2, the

decomposition temperature of the four elastomers about 300 °C show an upward trend as the catalyst content decreases, and the weight loss in the range of 300−400 °C, which has good thermal stability. This was attributed to the fact that the cross-linking density was increased as the catalyst content decreases when M:I was unchanged, M:C were changed, which will lead to promote hydrogen bonds and hydrophobic interactions were increased. Meanwhile, the energy of decomposition to destroy hydrogen bonding and hydrophobic association also was raised, resulting in the decomposition temperature is enhanced.

The T_g analysis

The plot of the loss factor (tan δ) against temperature indicates that the softening temperature of the elastomers are shown in Figure S3, the results showed that the peak of tanδ initially migrated to a high temperature with the decrease in catalyst content at a fixed frequency of 1 Hz, which may be explained by the reinforcement of the hydrophobic interactions and the stabilization of hydrogen bonds to activate the tanδ migrate to a high temperature. These results indicated that the T_g and strength of elastomers could be adjusted by the variation of the catalyst ratio. The elastomers showed the maximum softening temperature of 25.5 °C, below but close to 37 °C, thereby could be softened easily in 37 °C water (Figure 4A, Movie S3 (b)), suggesting an excellent body-temperature sensitivity.

The thermal transitions of the obtained elastomers are further studied by differential scanning calorimetry (DSC) experiments in the temperature range of -50-200 °C. The DSC thermograms of the monomer and initiator, and the crosslinked elastomer are shown in Figure S7 (a) and Figure S7 (b), respectively. The results show that the monomer shows the decomposition temperature (T_d) of 137.7 °C, the monomer and initiator exhibit the melting temperatures (T_m) of 75.9 and 62.3 °C,

66 respectively. After polymerization, the T_d and T_m of the monomer is disappeared, the T_m of initiator
67 is also disappeared, and indicating the monomer MBC had successfully ring-opened, without any
68 by-product. The obtained elastomers have a relatively high T_g of 23.6-26.6°C, and the T_g of the
69 elastomer slightly elevated as the content of catalyst is decreased. The T_g of the elastomers can be
70 adjusted by the variation of the catalyst ratio.

71 **The surface topography of self-healing analysis**

72 All samples were tested for optical microscope, and the procedure of self-healing at room
73 temperature, without requiring any external stimuli.

74 As shown in scratch tests (Figure S4), the P_2 as an example was discussed in detail. First,
75 repeatability tests were carried out in order to accurately quantify the self-healing efficiency, the
76 elastomer cylindrical (9 mm×9 mm) was cut into three completely separate pieces using a surgical
77 blade. Then, the self-healing of the every sample had been completely cut and had applied a slightly
78 force to dock softly the two cut interfaces. Second, a blade made 20-30 μm wide scratches on the
79 elastomer (Figure S4 (a)). Furthermore, optical microscopy images illustrated the artificial scratch
80 made on the surface of the P_2 almost completely self-healing within 3 h at room temperature (Figure
81 S4 (d)). The results showed that the scratch had basically healed and was consistent with the tensile
82 tests (Figure 5), this is because the non-covalent bonds between molecular chain segments are
83 rearranged at the fracture interface.

84 In order to further study the effect of higher physical crosslink density on the self-healing of
85 the obtained materials. The optical microscopy images and storage (G') modulus of the elastomer
86 P_4 are illustrated in Figure S8 and Figure S9, respectively. The self-healing efficiency of 92.1% of
87 the elastomer P_4, after self-healing 2 h (Figure S8), which shows that the higher physical cross-

linking density of the materials has better self-healing capability. Secondly, a blade made 20-30 μm wide scratches on the elastomer P_4 (Figure S9 (a)). The artificial scratch made on the surface of the P_4 almost completely self-healing within 2 h at room temperature (Figure S9 (d)). The results indicated that the scratch had basically healed and was consistent with the dynamic mechanical (Figure S8), which confirm further the higher physical cross-linking density of the materials to obtain better behavior, including better self-healing capability and faster the rearrangement of non-covalent bonds between molecular chain segments at the fracture interface.

Shape memory behavior analysis

Owing to the fact that the dual-physical cross-linked networks are introduced into the elastomers, it gives shape memory properties. The elastomers exhibited an outstanding self-recovery ability, the P_2 elastomer could recover its original state, and almost entirely within 2 min at room temperature after being stretched up to a given strain of 200% (Movie S1), without any environment treatment. The result showed that a potential the resistance of fatigue against repeated deformation. At the same time, self-recoverability was further evidenced by knotting, and no obvious residual strain was observed after unknotting and recovery to its original shape (Figure S5 (a)). Moreover, to further verify the ability of self-healing, reprogramming the permanent shape of the elastomers were performed. The detailed procedure to reprogram these new permanent shape “N, E, U” from the permanent linear shape (Figure S5 (b)). The original linear shape was erased after the reprogramming, the new reprogramming shape was formed (Movie S2 (a)). Then, The reprogramming of permanent shape was established by the re-association of hydrophobic interactions and the re-form of hydrogen bonds at room temperature. The self-recoverability of new shapes was demonstrated by knotting, and the reprogramming of permanent shape of the elastomers

could be quickly recovered within 2 min at room temperature (as an example, E shape was performed, Movie S2 (b)).

To qualitatively evaluate the shape memory properties and temperature responsiveness, P_1-P_4 was made into 3 cm rod-shaped materials, and the plasticity was U-shaped under external force. [1-4] As shown in Figure 6 (a) and Movie S3 (a), Movie S3 (b), the P_2 elastomer was put into 7 ^oC ice water to fix shape for 10 s, and a 40 g weight was loaded for 10 s without deformation. Then, the fixed shape was immersed in 37 ^oC water for 10 s. The results showed that the elongation of P_2 was 100% it could happen in response to human body-temperature, which was attributed to the temperature dependence of hydrogen bonds and hydrophobic associations of the dual-physical cross-linked network structure.

The quantitative evaluation of the shape memory behavior of the elastomer P_2 is obtained by dynamic thermodynamic analysis on a DMA (Q800, TA Instrument) to qualitatively evaluate further the shape memory behavior of the obtained materials and temperature responsiveness. As illustrated in Figure S 10, the dual-shape memory cycle of the obtained materials. The sample with cylindrical (ca. 6.000 mm (W) × 3 cm (L)) is uniaxially stretched to a strain of 40% at 15 ^oC and followed shape fixation at 28 °C for 1h. The results indicate that a fixation ratio of R_f =79.5±2.6% and a recovery ratio of R_r=94.0±2.0%, which would offer a guideline to synthesize high-performance shape memory materials.

Supporting Figures

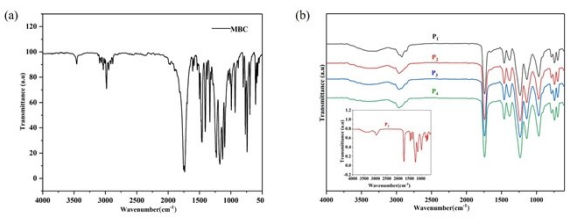

Figure S1 (a). FTIR spectra of the monomer. (b). FTIR spectra of the elastomers.

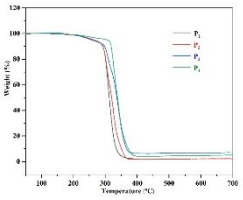

Figure S2. Thermogravimetric analysis of the elastomers

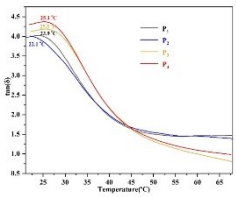

Figure S3. The loss factor (tan δ) as a function of temperature for elastomers.

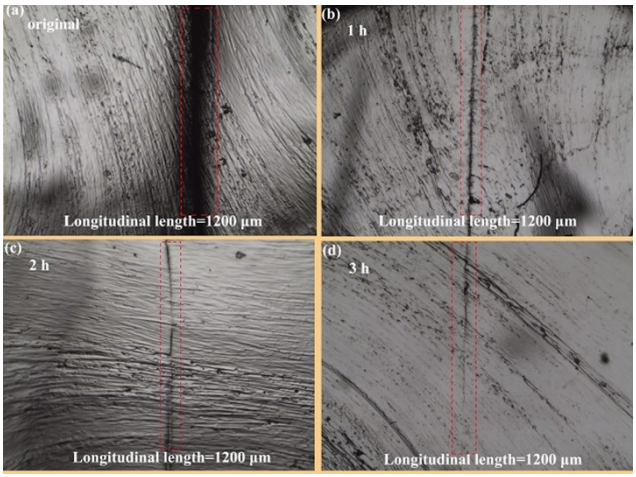

Figure S4 Optical microscopy images of the P_2 elastomer after being scratched. It showed a rapid self-healing with an almost complete recovery within 3 h at room temperature

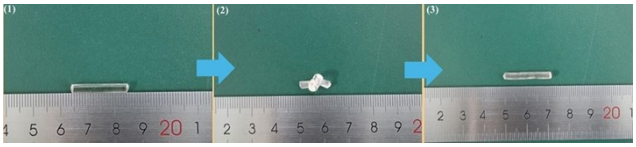

Figure S5 Images demonstrate the full recovery of a P_2 sample (size: 2.2 cm ×3mm) after knotting without any break

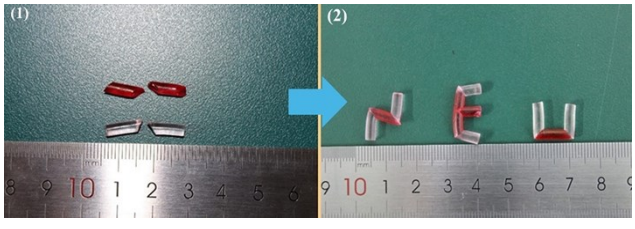

Figure S6 Images demonstrate the full recovery of a P_2 sample (size: 2.2 cm ×3mm) after self-healing without any break

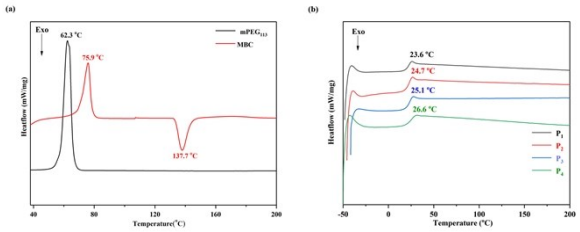

Figure S7. (a) DSC curves of the monomer and initiator; (b) DSC curves of the obtained elastomers.

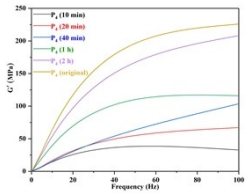

Figure S8. The storage (G') modulus of the elastomer P_4 with different self-healing time.

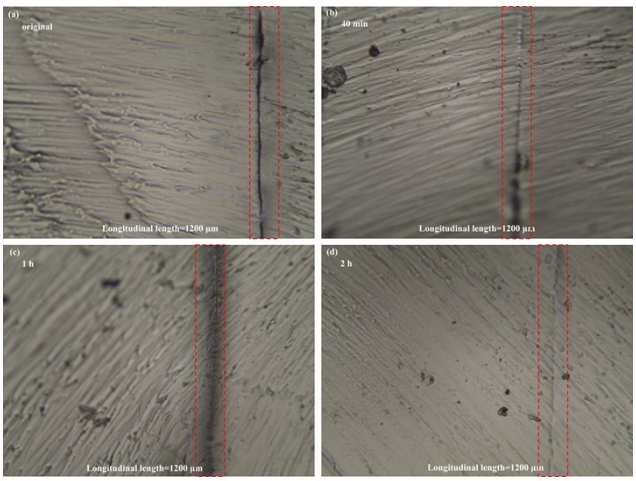

Figure S9 Optical microscopy images of the P_4 elastomer after being scratched. It showed a rapid

157 self-healing with an almost complete recovery within 2 h at room temperature

158

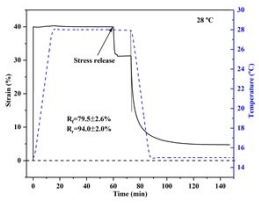

159

160 Figure S10 Shape memory behavior of the P_2 elastomer

161 **Table S1**. Polymer Density, Swelling Ratio, and Cross-Linking Density of P_1-P_4 Sample[a]

Samples	Polymer density (g/cm^3)	Swelling ratio (%)	Cross-linking density ($10^{-4}mol/cm^3$)
P_1	0.66± 0.01	302.3 ± 1.2	3.87 ± 0.05
P_2	0.78± 0.08	229.7 ± 0.7	5.36 ± 0.02
P_3	0.80± 0.02	182.2 ± 0.3	7.93 ± 0.01
P_4	0.84± 0.06	143.2 ± 0.5	11.3 ± 0.03

162 [a]The error in the table is standard deviation (3 specimens for each sample)

163

164 **Table S2.** Mechanical properties of elastomers with different catalyst content.

Samples	Elongation at break (%)	Young's modulus (MPa)	Tensile strength(MPa)
P_1	236.64± 11.00	4.43±0.18	10.50±0.25
P_2	301.76± 8.61	4.13± 0.18	14.61±0.67
P_3	407.37± 7.99	3.72± 0.23	14.88±0.6
P_4	409.70± 5.97	3.66± 0.19	15.49±0.9

Table S3. Mechanical properties of the obtained elastomers exceeds almost all previously reported room-temperature elastomers

Reference	Maximum modulus(MPa)	Maximum tensile strength(MPa)	Journals
[3]	3	-	*Nature*., 2010,
[8]	0.1	-	*Adv. Mater*., 2009
[17]	80	0.15	*Adv. Mater.,* 2016
[18]	0.1	0.28	*Adv. Funct. Mater.,* 2015
[19]	175	5.1±0.16	*ACS. App. Mater. Inter*., 2019
[20]	0.6	0.06	*ACS. Macro. Lett*., 2012
[24]	-	14.8	*Adv. Mater*., 2019
[26]	0.01	6.8	*Adv. Mater*., 2018
[35]	1.0	3.5	*Macromolecules*., 2016
[38]	10	4.5	*Adv. Funct. Mater.,* 2020
[42]	0.1	1.5	*Macromolecules*., 2016

Reference

[1] Q. Zhao, H. J. Qi and T. Xie, *Prog. Polym. Sci.,* 2015, **49**, 79-120.

[2] Q. Zhao, W. Zou, Y. Luo and T. Xie, *Sci. Adv.,* 2016, **2**, e1501297.

[4] R. Liang, H. Yu, L. Wang, L. Lin, N. Wang and K. U. R. Naveed, *ACS. App. Mater. Inter*., 2019, **11**, 43563-43572.

[5] Y. K. Bai, J. W. Zhang and X. Chen, *ACS. App. Mater. Inter*., 2018, **10**, 14017-14025.